contribution also enters through the quantities δ^* and δ_p, and these quantities are based on boundary-layer profiles which have also, implicitly, included the effect of blowing (or suction) through the appropriate boundary conditions used in solving the boundary-layer equations.

For flows with moderate Mach numbers $[M_\infty^2 \simeq 0(1)]$, the additional term $\rho_w v_w/\rho_\infty U_\infty$, may have significant contributions to the displacement thickness, because its magnitude may well be comparable to that of the term $\partial\delta^*/\partial x$.

For nearly quasi-steady hypersonic flows with "similarity type" of blowing (or suction), i.e. $\rho_w v_w/\rho_\infty U_\infty = \alpha/(Re)^{\frac{1}{2}}$, as treated in [6], this additional term is found to be small compared to $\partial\delta^*/\partial x$; however, it may become comparable to the term $U_\infty^{-1}(\partial\delta_p/\partial t)$, depending on the parameters characterizing the flow unsteadiness. A discussion on boundary layer induced pressures for such flows also appears in [6].

Finally we remark that the idea used in this note can be employed to generalize the study to more general flow configurations. Thus in two dimensional flow, for example, we shall have the situations of $U_\infty = U_\infty(x, t)$, $\rho_\infty = \rho_\infty(x, t)$ for an arbitrary body in unsteady motion.

ACKNOWLEDGEMENTS

This work was supported by the Air Force Office of Scientific Research (AFOSR) under Grant AF-AFOSR-68-1581. The author acknowledges some helpful comments of E. Reshotko.

REFERENCES

1. W. D. HAYES and R. F. PROBSTEIN, *Hypersonic Flow Theory*, Chapter 9, 1st edn. Academic Press, New York (1959).
2. H. SCHLICHTING, *Boundary Layer Theory*, (English Translation by J. KESTIN), Chapter 2, 4th edn. McGraw-Hill, New York (1960).
3. F. K. MOORE and S. OSTRACH, Displacement thickness of the unsteady boundary layers, *J. Aeronaut. Sci.* **24**, 77–78 (1957).
4. W. M. MANN, JR., Effective displacement thickness for boundary layers with surface mass transfer, *AIAA Jl* **1**, 1181–1182 (1963).
5. N. HAYASI, Displacement thickness of the boundary layer with blowing, *AIAA Jl* **3**, 2348–2349 (1965).
6. T. F. ZIEN, Unsteady, compressible boundary layers on a flat plate with mass transfer, to appear as an AFOSR-Case Western Reserve University Report, AFOSR 69-2707 TR (1969).
7. T. F. ZIEN and E. RESHOTKO, Boundary layer induced pressures on a flat plate in hypersonic flight, AFOSR Scientific Report 69-1229 TR, (May 1969). Case Western Reserve University FTAS/TR-69-43. Also, *AIAA Jl* **8**, 158–160 (1970).

Int. J. Heat Mass Transfer. Vol. 13, pp. 1371–1375. Pergamon Press 1970. Printed in Great Britain

EXTENSION OF THE NUMERICAL METHOD FOR MELTING AND FREEZING PROBLEMS

W. L. HEITZ* and J. W. WESTWATER
Division of Chemical Engineering, University of Illinois, Urbana, Illinois, U.S.A.

(*Received* 19 *January* 1970)

NOMENCLATURE

- D, horizontal dimension of test cell [cm];
- E, vertical dimension of test cell [cm];
- k, thermal conductivity [cal/cms °C];
- k_{eff}, effective thermal conductivity [cal/cms °C];
- L, vertical dimension of liquid [cm];
- n, nodal position in space network;
- N, total number of space nodes;
- Nu, Nusselt number, k_{eff}/k_2 [dimensionless];
- Q, heat flux [cal/cm^2 s];
- r, number of spatial node at solid–liquid interface;
- t, time [s];
- T, temperature [°C];
- T_F, fusion temperature [°C];
- u, velocity [cm/s];
- x, distance along vertical axis [cm].

Greek symbols
- α, thermal diffusivity [cm^2/s];
- ϵ, ice thickness, interface position [cm];
- θ, point temperature minus fusion temperature, $T - T_F$ [°C];
- λ, latent heat of fusion [cal/g];
- ρ, density [g/cm^3].

* Present address: Shell Development Company, Emeryville, California.

Subscripts
1, solid phase;
2, liquid phase;
m, number of time incrpments;
n, position of spatial node;
0, initial condition.

INTRODUCTION

THE MATHEMATICAL description of the rate of solid–liquid phase change during unidirectional heat transfer in the direction of gravity has been presented using numerous techniques. A powerful method is numerical integration. The finite-difference method of Murray and Landis [1] is particularly useful.

The differential equations describe conduction in the solid phase:

$$\frac{\delta\theta_1}{\delta t} = \alpha_1 \frac{\delta^2\theta_1}{\delta x^2} \tag{1}$$

and conduction in the liquid phase:

$$\frac{\delta\theta_2}{\delta t} = \alpha_2 \frac{\delta^2\theta_2}{\delta x^2}. \tag{2}$$

These are coupled by a heat balance at the interface:

$$\lambda\rho_1 \frac{\delta\epsilon}{\delta t} = k_1 \frac{\delta\theta_1}{\delta x}\bigg|_\epsilon - k_2 \frac{\delta\theta_2}{\delta x}\bigg|_\epsilon. \tag{3}$$

The Murray–Landis scheme uses a variable-space network such that each phase is divided into equal-size space increments which change in size as the fusion front moves. The above equations are written in difference form using a three-point temperature approximation. Equation (4) applies for $0 \leqslant n \leqslant r$, and equation (5) is for $r \leqslant n \leqslant N$.

$$\frac{\theta_{n,m+1} - \theta_{n,m}}{\Delta t} = \frac{n}{\epsilon}\left[\frac{(\theta_{n+1,m} - \theta_{n-1,m})}{2}\frac{\Delta\epsilon}{\Delta t}\bigg|_m\right] + \frac{\alpha_1 r^2}{\epsilon^2}(\theta_{n-1,m} - 2\theta_{n,m} + \theta_{n+1,m}) \tag{4}$$

$$\frac{\theta_{n,m+1} - \theta_{n,m}}{\Delta t} = \frac{N-n}{E-\epsilon}\left[\frac{(\theta_{n+1,m} - \theta_{n-1,m})}{2}\frac{\Delta\epsilon}{\Delta t}\bigg|_m\right] + \alpha_2\left(\frac{N-r}{E-\epsilon}\right)^2(\theta_{n-1,m} - 2\theta_{n,m} + \theta_{m+1,m}) \tag{5}$$

$$\lambda\rho_1 \frac{\Delta\epsilon}{\Delta t}\bigg|_m = \frac{k_1 r}{2\epsilon}(\theta_{r-2,m} - 4\theta_{r-1,m}) + \frac{k_2(N-r)}{2(E-\epsilon)}(\theta_{r+2,m} - 4\theta_{r+1,m}). \tag{6}$$

If initial and boundary conditions are specified, the equations can be solved on a digital computer for interfacial position and velocity and the temperature profile as a function of time.

Thomas and Westwater [2] verified the model using their experimental data for n-octadecane. The model was extended to include free convection in the liquid by Boger and Westwater [3], and verification was obtained with their data for water. Additional extensions are reported in this communication. New data were obtained [4] using apparatus similar to that used by these prior workers. Pure water was confined in transparent plastic cells, 1·27 × 1·27 cm square, with heights of 3–10 cm. Heat transfer was vertical. The interfacial motion was obtained by cinephotomicroscopy, and the temperature profile was obtained with thermocouples.

DEFINING THE SOLUTION WHEN ONE PHASE IS INITIALLY PRESENT

If only one phase is present initially, either ϵ or $E - \epsilon$ is zero and equations (4) and (6) or (5) and (6) are undefined. The starting procedure (Method I) used earlier [3] assumed that for a short starting time the latent heat transfer in water was equal to the sensible heat change in the heat sink (a cooled copper block) at one end of the cell. This arbitrary scheme prevents wild starting values. Although initial velocities of incorrect sign can result, agreement was obtained between experimental data and the model shortly thereafter.

An improved starting procedure (Method II) has been developed which gives initial velocities of correct sign. The liquid is considered to be effectively infinite in depth at the start of a freezing test. A small time increment t_0 is selected, and the sensible heat removed (resulting in subcooled liquid) during that time is computed using the well-known [5] expression:

$$\int_0^{t_0} Q\,\mathrm{d}t = 2k_2\,[T_F - T_1(0, t_0)]\,\sqrt{(t_0/\pi\alpha_2)}. \tag{7}$$

One assumes that all the sensible heat of subcooling is then converted instantly to latent heat change resulting in a solid thickness ϵ_0 at time t_0 given by:

$$\epsilon_0 = \frac{2k_2}{\lambda\rho_1}[T_F - T_1(0, t_0)]\,\sqrt{(t_0/\pi\alpha_2)}. \tag{8}$$

This value of ϵ_0 is used to start the difference equations, and elapsed time thereafter is added to t_0. A similar procedure is used if only solid is initially present. In general it is necessary only to obtain a realistic starting thickness and not an accurate value, because the time t_0 is a negligible fraction of the total time. Thus, corrections for sensible heat residing in the solid and liquid at time t_0 are seldom justified. Similarly, the assumption of a linear profile in the solid at t_0 is satisfactory.

Methods I and II are compared in Fig. 1. Curves 2 and 4 indicate that little change results if ϵ_0 is decreased from the theoretical value of 0·2 cm to 0·091 (an arbitrary value which could result if sensible heats were considered). Curve 3 is in

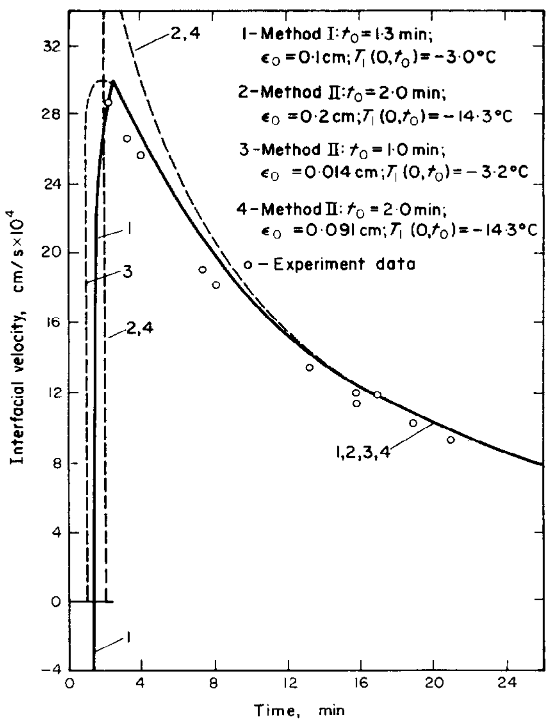

FIG. 1. Comparison of starting methods when only one phase is initially present. Run 3H, water at 12·5°C initially present, freezing initiated at top by decreasing top temperature to −42·5°C, cell height of 4·59 cm.

better agreement with experimental data; this is expected since $T_1(0, t_0)$ is nearer T_F and errors introduced by the assumptions are smaller.

EFFECT OF UNEQUAL PHASE DENSITIES

During any phase change for which the densities of the two phases differ, fluid motion occurs. For the water–ice system the direction is away from the ice during freezing and towards the ice during melting. The velocity of the drift was expressed by Longwell [6] and Scriven [7] but its use for melting and freezing has been omitted till now. The drift depends on the densities as shown by a mass balance at the interface:

$$u_2 = \left(\frac{\rho_2 - \rho_1}{\rho_2}\right)\frac{d\epsilon}{dt}. \tag{9}$$

Assuming λ is evaluated at T_F, equation (3) is unchanged. Equation (2) becomes:

$$\frac{\delta\theta_2}{\delta t} + \frac{\delta\theta_2}{\delta x}\frac{(\rho_2 - \rho_1)}{\rho_2}\frac{d\epsilon}{dt} = \alpha_2\frac{\delta^2\theta_2}{\delta x^2}. \tag{10}$$

Figure 2 shows a comparison of the mathematical solutions with equal and unequal phase densities. Since both solutions yield the same final interfacial position, lower interfacial velocities at early times for the second solution result in higher velocities later in the run. The solution using differing densities is in better agreement with the data, although the effect is small. The magnitude of the effect depends on the ratio of heat transport in the liquid by conduction to the transport by liquid drift. The effect will be important for large interfacial velocities or large density differences. Note that the liquid motion considered here is not caused by buoyancy and is not free convection as generally understood. If free convection occurs, the procedure is modified as described below.

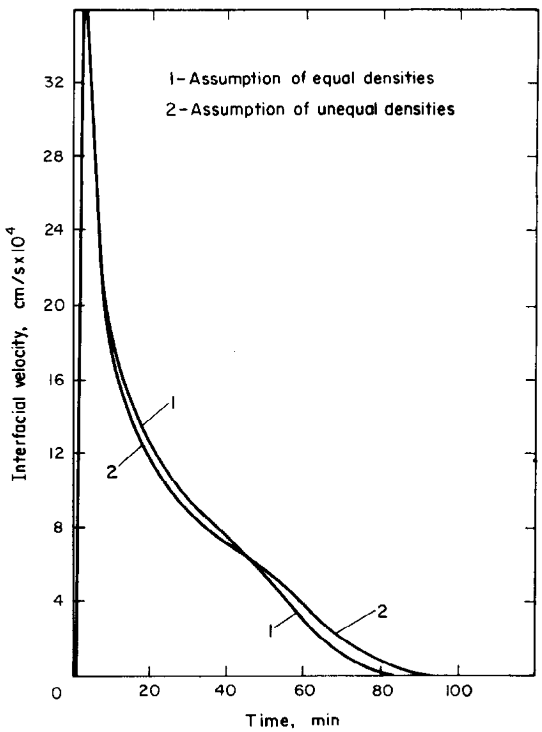

FIG. 2. Effect of unequal phase densities. Run 3D, water at 13·8°C initially present, freezing initiated at top by decreasing top temperature to −46·5°C, cell height of 4·59 cm.

EFFECT OF LIQUID L/D DURING NATURAL CONVECTION

Inasmuch as no analytical solution is available for the effect of natural convection due to buoyancy forces in the liquid, the use of an empirical effective conductivity has been

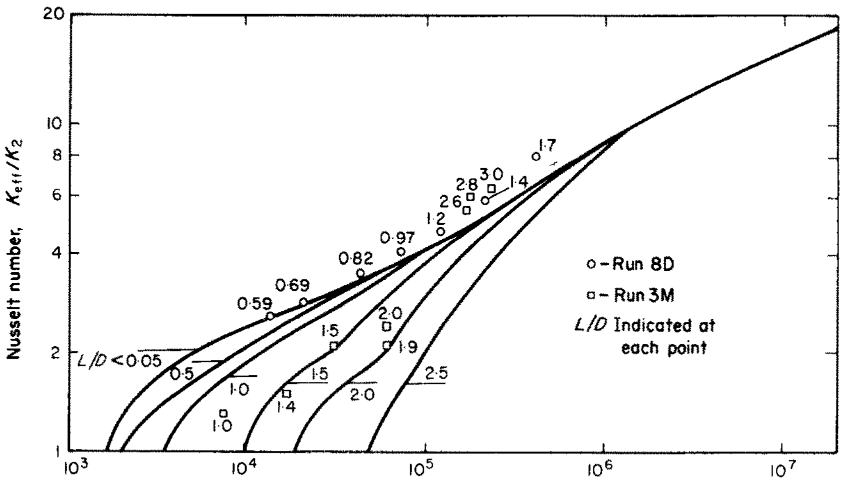

FIG. 3. Comparison of transient data with steady-state correlation of Nusselt numbers vs. Rayleigh number; depth–width ratio (L/D) of liquid included.

adopted. This accounts for heat transport by both conduction and convection. Boger and Westwater [3] showed that transient data for melting and freezing agreed with non-phase-change data of Globe and Dropkin [8] and Schmidt and Silveston [9]. A good correlation of all these data is given by O'Toole and Silveston [10] and is shown as the upper curve in Fig. 3. The effect of the depth–width ratio (L/D) of the liquid was neglected. The value was below 0·5.

The recent tests (non-phase-change) of Catton and Edwards [11] show that L/D is an important parameter during natural convection. Their results are the family of curves in Fig. 3. The transitions from pure conduction

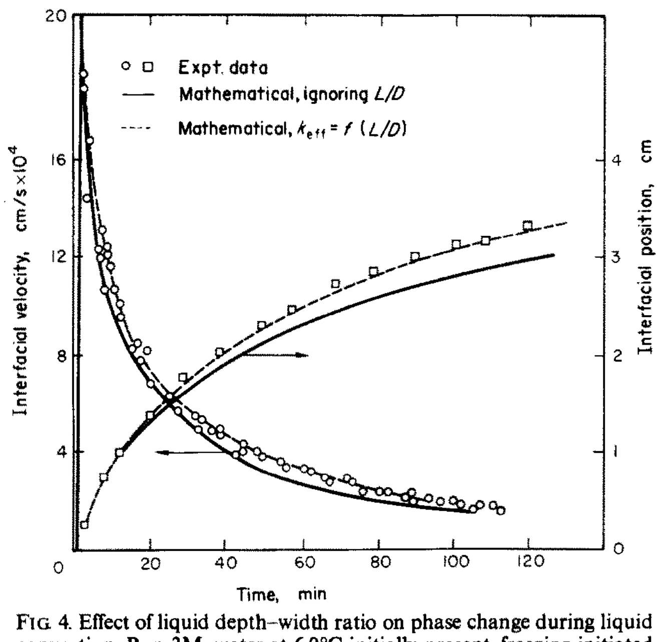

FIG. 4. Effect of liquid depth–width ratio on phase change during liquid convection. Run 3M, water at 6·9°C initially present, freezing initiated at top by decreasing top temperature to −16°C. cell height of 48·6 cm.

($Nu = 1$) to convection ($Nu > 1$) were verified in the present study for L/D of 0·5 and 1·0. Transient data obtained during phase change are shown in Fig. 3 and these substantiate the effect of L/D in the range of 0·59–3·0.

Experimental interfacial velocities and positions are given in Fig. 4. Also shown are predicted results using k_{eff} as a function of L/D in the finite-difference equations. The agreement is superior to that obtained when the effect of L/D is ignored.

In summary, the additional uses of the numerical method of Murray and Landis now include (1) Cases in which only one phase is present initially; (2) Cases with unequal densities for the phases; (3) Cases with free convection in the liquid; and (4) Cases such that the depth-width ratio for the liquid affects convection in the liquid.

ACKNOWLEDGEMENTS

A NASA Traineeship, a Dow Chemical Company Fellowship and a National Science Foundation Grant supported this research.

REFERENCES

1. W. D. Murray and F. Landis, Numerical and machine solutions of transient heat conduction problems involving phase change, *J. Heat Transfer* **81**, 106–112 (1959).
2. L. J. Thomas and J. W. Westwater, Microscopic study of solid–liquid interfaces during melting and freezing, *Chem. Engng Prog. Symp. Ser.* **59**, No. 41, 155–164 (1963).
3. D. V. Boger and J. W. Westwater, Effect of buoyancy on the melting and freezing process, *J. Heat Transfer* **89**, 81–89 (1967).
4. W. L. Heitz, Hydrodynamic stability of water and its effect on melting and freezing, Ph.D. Thesis, University of Illinois, Urbana, Illinois (1970).
5. E. R. G. Eckert and R. M. Drake, Jr., *Heat and Mass Transfer*. McGraw-Hill, New York (1959).
6. P. A. Longwell, Graphical method for solution of freezing problems, *J. Am. Inst. Chem. Engrs* **4**, 53–57 (1958).
7. L. E. Scriven, On the dynamics of phase growth, *Chem. Engng Sci.* **10**, 1–13 (1959).
8. S. Globe and D. Dropkin, Natural-convection heat transfer in liquids confined by two horizontal plates and heated from below, *J. Heat Transfer* **81**, 24–28 (1959).
9. E. Schmidt and P. L. Silveston, Natural convection in horizontal liquid layers, *Chem. Engng Prog. Symp. Ser.* **55**, No. 29, 163–169 (1959).
10. J. L. O'Toole and P. L. Silveston, Correlations of convective heat transfer in confined horizontal layers, *Chem. Engng Prog. Symp. Ser.* **57**, No. 32, 81–86 (1961).
11. I. Catton and D. K. Edwards, Effect of side walls on natural convection between horizontal plates heated from below, *J. Heat Transfer* **89**, 295–299 (1967).

Int. J. Heat Mass Transfer. Vol. 13, pp. 1375–1378. Pergamon Press 1970. Printed in Great Britain

STEADY STATE TEMPERATURE PROFILES WITHIN INSULATED ELECTRICAL CABLES HAVING VARIABLE CONDUCTIVITIES

DONALD S. COHEN* and FREDRICK H. SHAIR†

Departments of Applied Mathematics and Chemical Engineering, California Institute of Technology, Pasadena, California, U.S.A.

(*Received* 16 *May* 1969 *and in revised form* 5 *February* 1970)

NOMENCLATURE

E, electric field;
C_0, constant defined by equation (6);
f_1, defined by equation (18);
f_2, defined by equation (19);
f_3, solution of equation (16);
g_0, defined by equation (39);
g_1, defined by equation (40);
g_2, solution of equation (36);
h, $\gamma/\ln \eta_0$;
J, Joule heating parameter, $\sigma_0 E^2 r_c^2/k_0 T_0$;
k, thermal conductivity of conductor at temperature T;
k_0, thermal conductivity of conductor at temperature T_0;
k_i, thermal conductivity of insulator;
r, radial coordinate measured from center of conductor;
r_c, radius of conductor;
r_0, radial distance from center of conductor to outside surface of insulator;
T, temperature;
T_0, temperature of outside surface of insulator.

* Partially supported by the U.S. Army Research Office (Durham) under Contract DAHC 04-68-C-0006.

† Partially supported by AEC Contract AT(04-3)767.